

Supporting information

Highly efficient charge transfer through double Z-scheme mechanism by Cu promoted MoO₃/g-C₃N₄ hybrid nanocomposite with superior electrochemical and photocatalytic performance

Sulagna Patnaik^a, Gayatri Swain^a, K. M. Parida^{a*}

^aCentre for Nano Science and Nanotechnology, Siksha O Anusandhan (Deemed to be University), Bhubanswar-751030, Odisha, India

Corresponding Author:

***E-mail:** kulamaniparida@soauniversity.ac.in

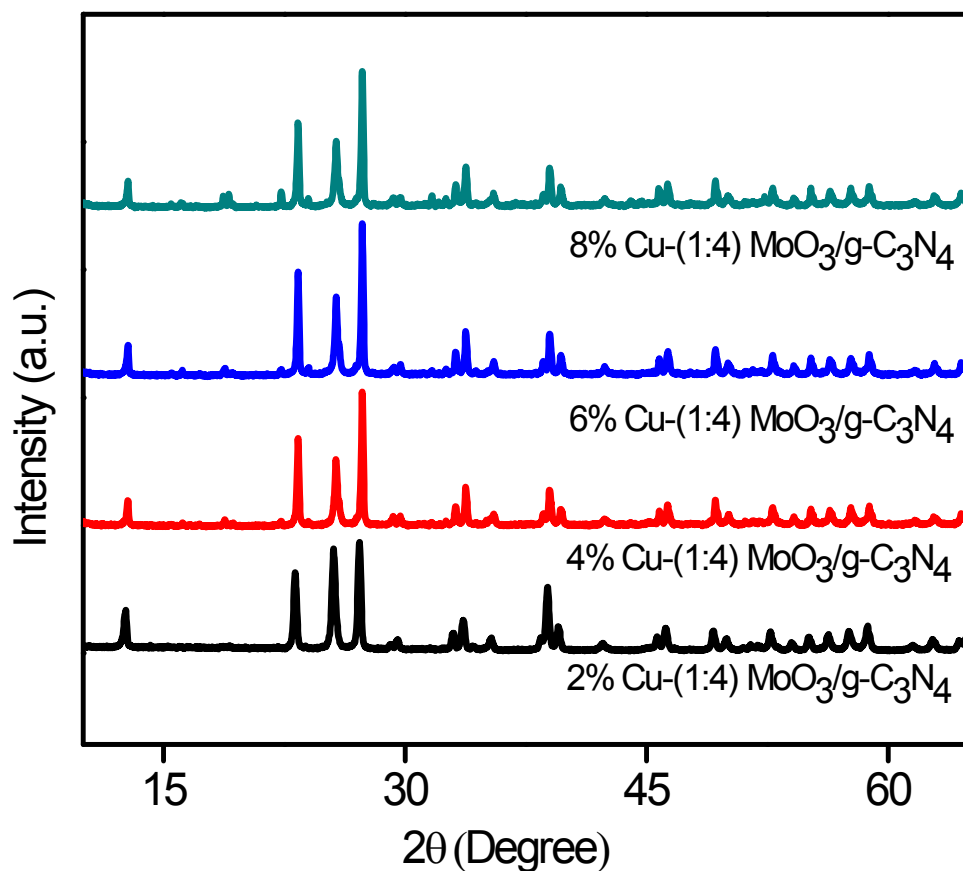


Figure S1. XRD spectra of MoO₃/g-C₃N₄ composite containing different content of Cu

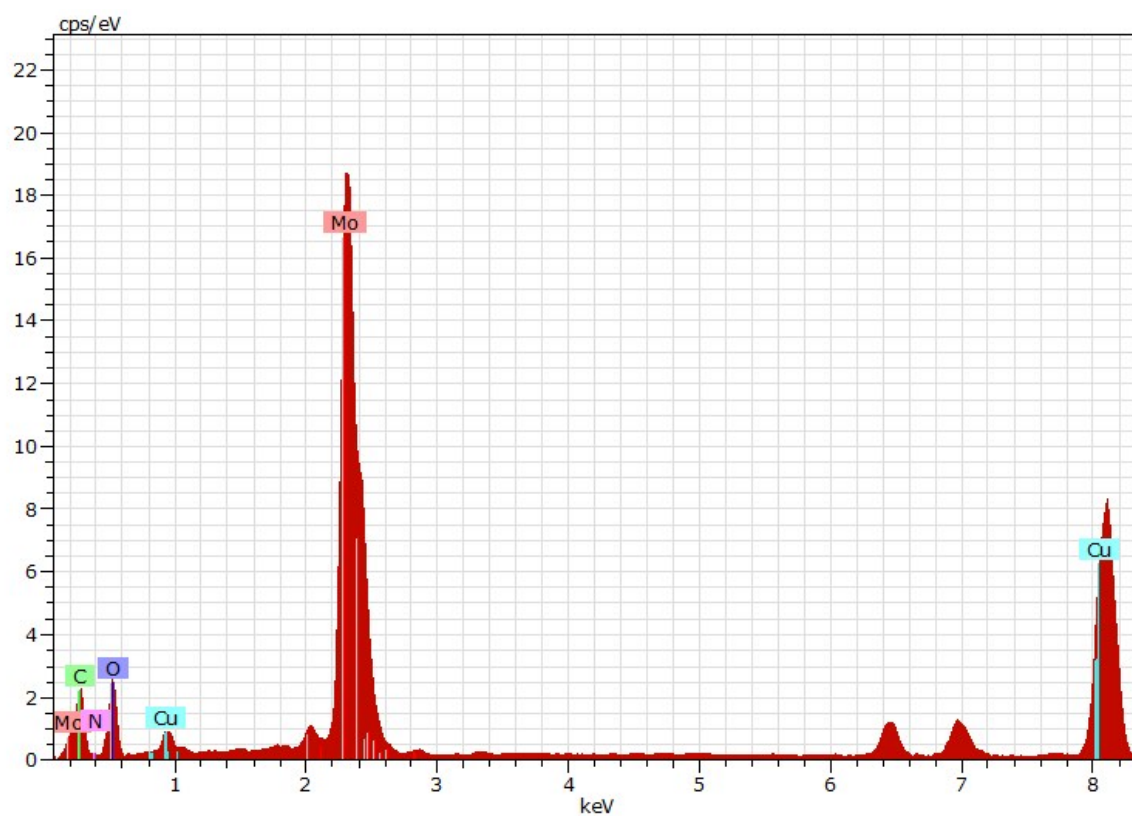


Figure S2. EDS of different elements present in the Cu-MoO₃/g-C₃N₄

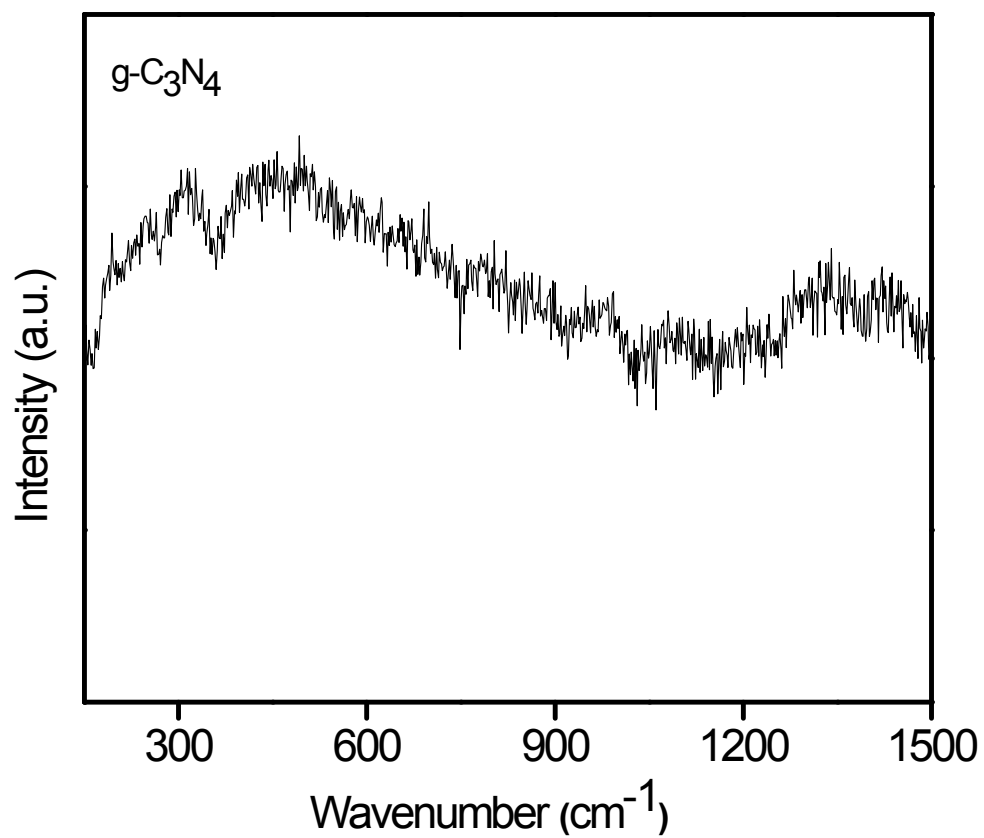


Figure S3. Raman spectra of neat g-C₃N₄

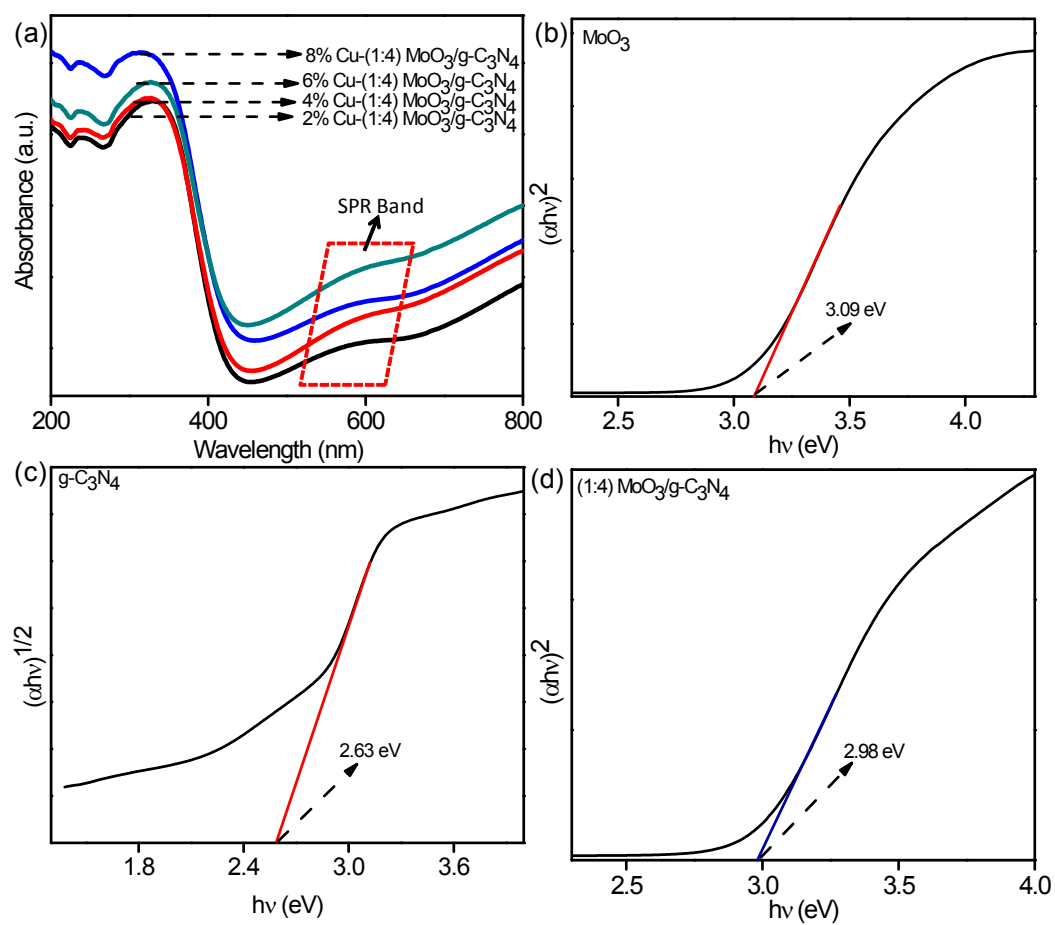


Figure S4. (a) UV-Vis absorption spectra of various percentage of Cu loading MoO₃/g-C₃N₄ composite and Band gap potential of (b) MoO₃, (c) g-C₃N₄ and (d) (1:4) MoO₃/g-C₃N₄

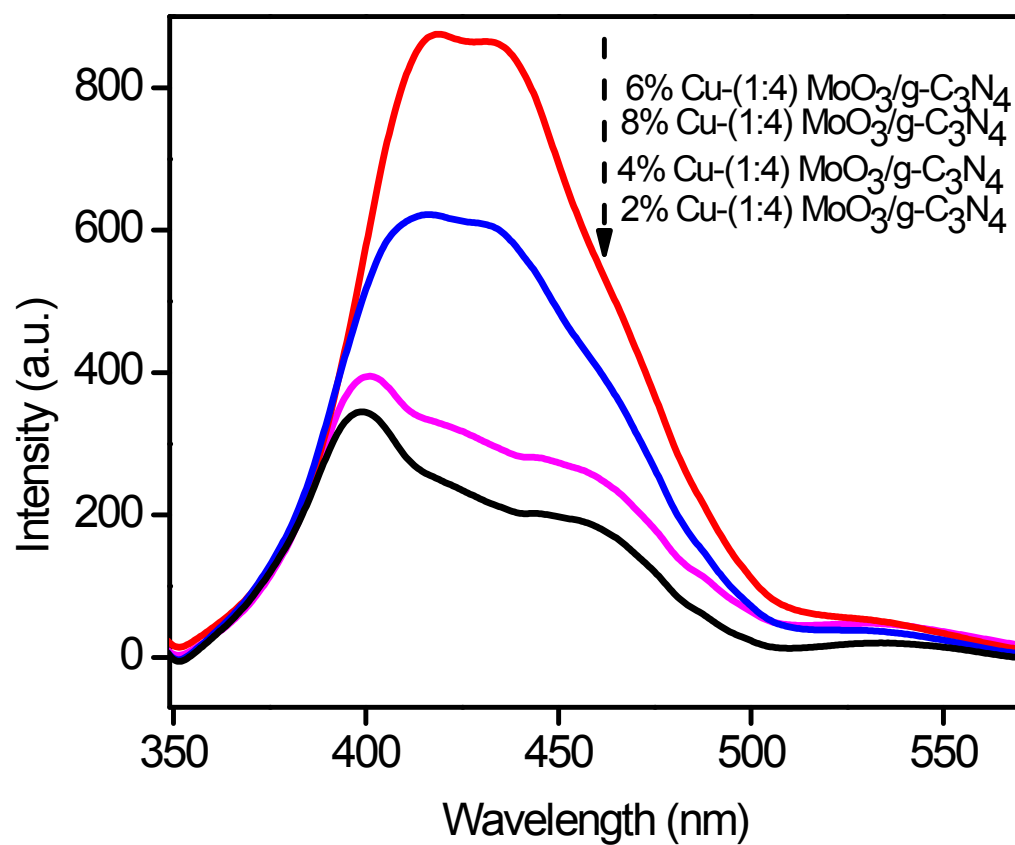


Figure S5. PL spectra of MoO₃/g-C₃N₄ composite with different amount of Cu

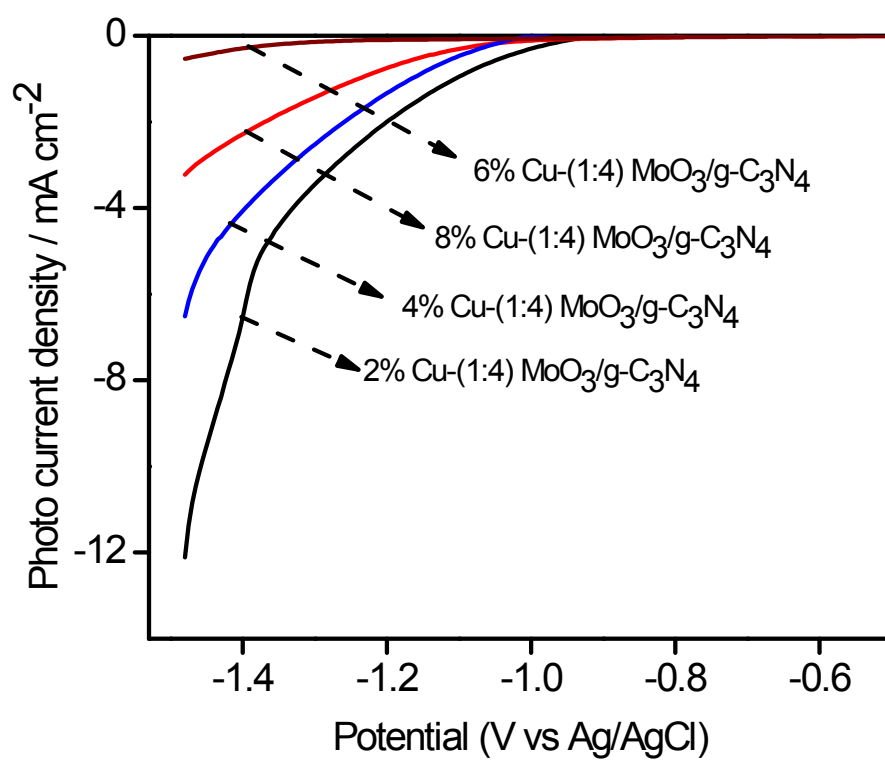


Figure S6. LSV plot of various weight % of Cu loading MoO₃/g-C₃N₄

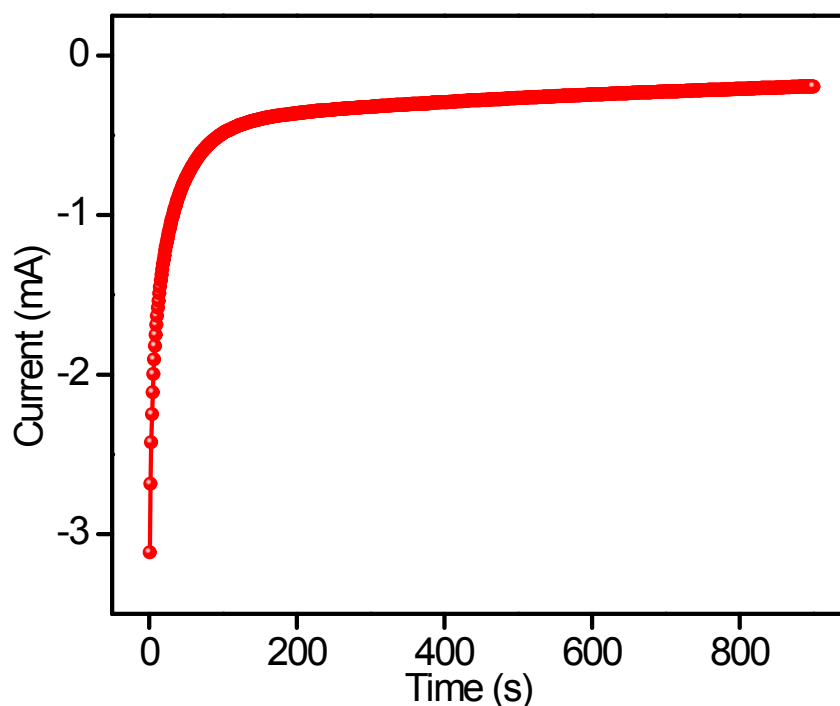


Figure S7. Chronoamperometry test for 2%Cu-(1:4)MoO₃/g-C₃N₄ at -1.30 applied potential

Electrochemical stability

In order to investigate the stability of the electrocatalytic activity chronoamperometry was carried for 900s. Figure S7 shows the corresponding chronomperometric response of time dependence cathodic photocurrent of Cu-MoO₃/g-C₃N₄ electrodes in 0.5 M Na₂SO₄ solution (pH = 6.3) at -1.30 V applied potential Vs. Ag/AgCl. When the photocatalyst was irradiated with light, the cathodic photocurrent rapidly increased at the initial stage and then became relatively stable with time. The current density exhibits a very slow attenuation and a high relative current of 65% still persists even after 900s [1].

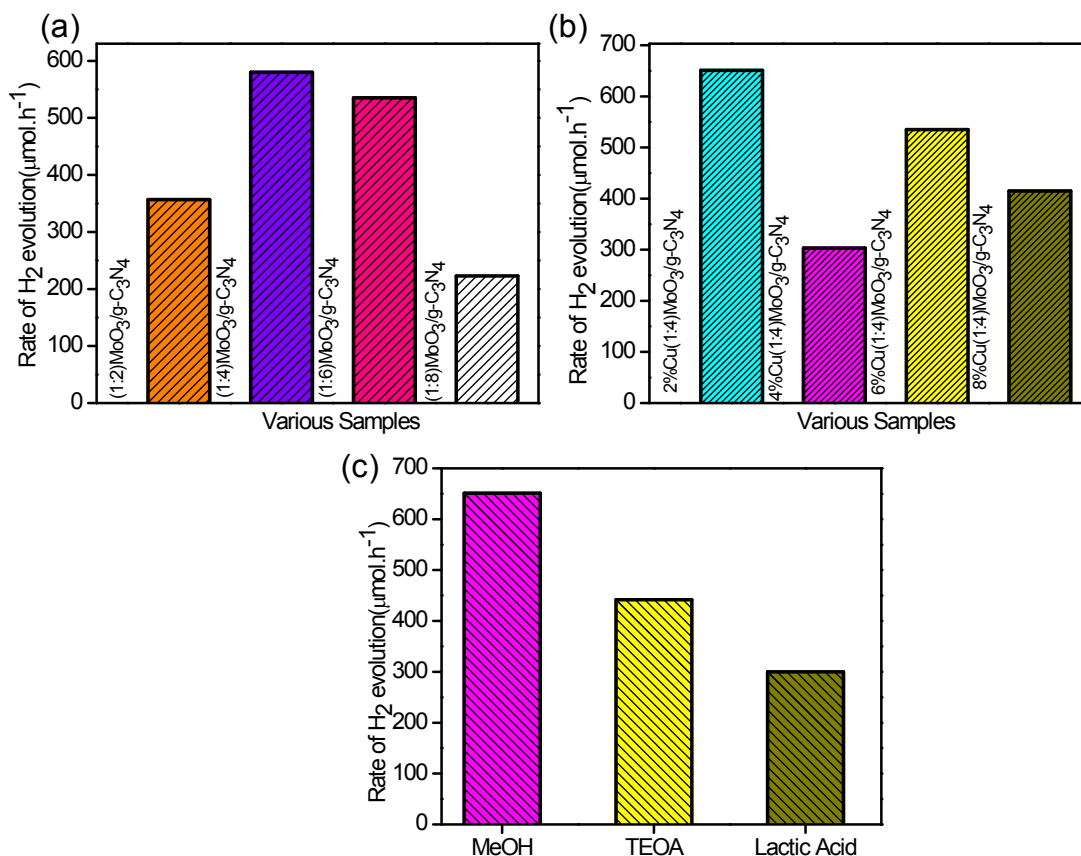
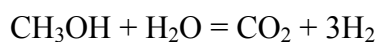


Figure S8. Hydrogen evolution study of (a) various weight percentages of MoO₃/g-C₃N₄ and (b) Cu loaded MoO₃/g-C₃N₄ (c) H₂ evolution study of 2% Cu-(1:4) MoO₃/ g-C₃N₄ composite using various scavenger component

Actually sacrificial agents play a decisive role in H₂ evolution because they act as electron donors and consume the photogenerated holes during photo catalytic reaction. To compare the effect of various sacrificial agents oxidation potentials are important. However, along with oxidation potential, permittivity and chain length in case of organic sacrificial agents also affect the rate of H₂ evolution [2]. In the present study, all the three factors are responsible for enhanced H₂ evolution rate of Cu-MoO₃/g-C₃N₄ composite in presence of methanol. It should be noted that, in the case of using 20% methanol solution as the electron donor, H₂ is also produced from water as a result of methanol conversion according to the following equation [3]



Moreover, the presence of oxygen vacancy defects of MoO_3 strongly enhances interactions, because of electron back-donation from surface Mo^{3+} into the π^* orbital of molecular CO and methanol get oxidized to CO_2 easily [4].

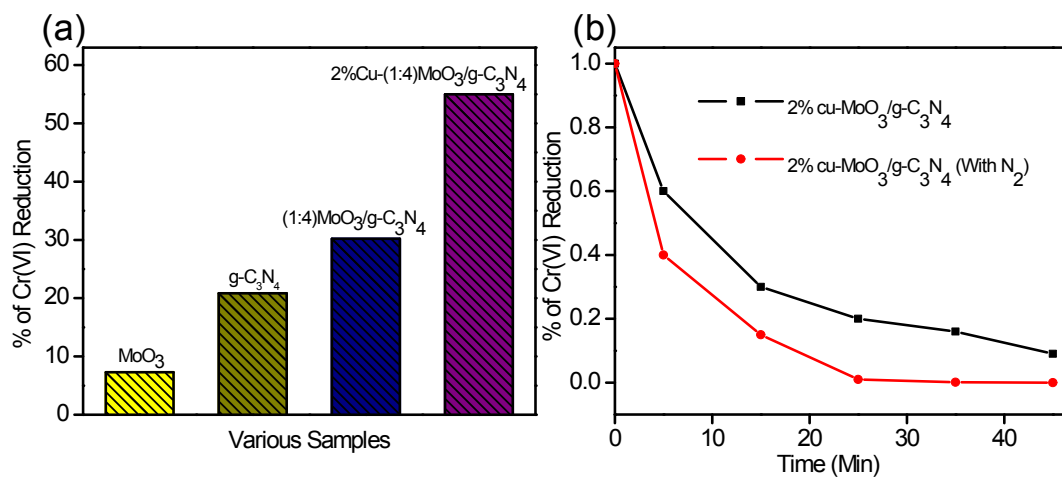


Figure S9. (a) Reduction of Cr(VI) by neat and composite sample (b) Photoreduction of Cr (VI) in the presence of N_2 gas

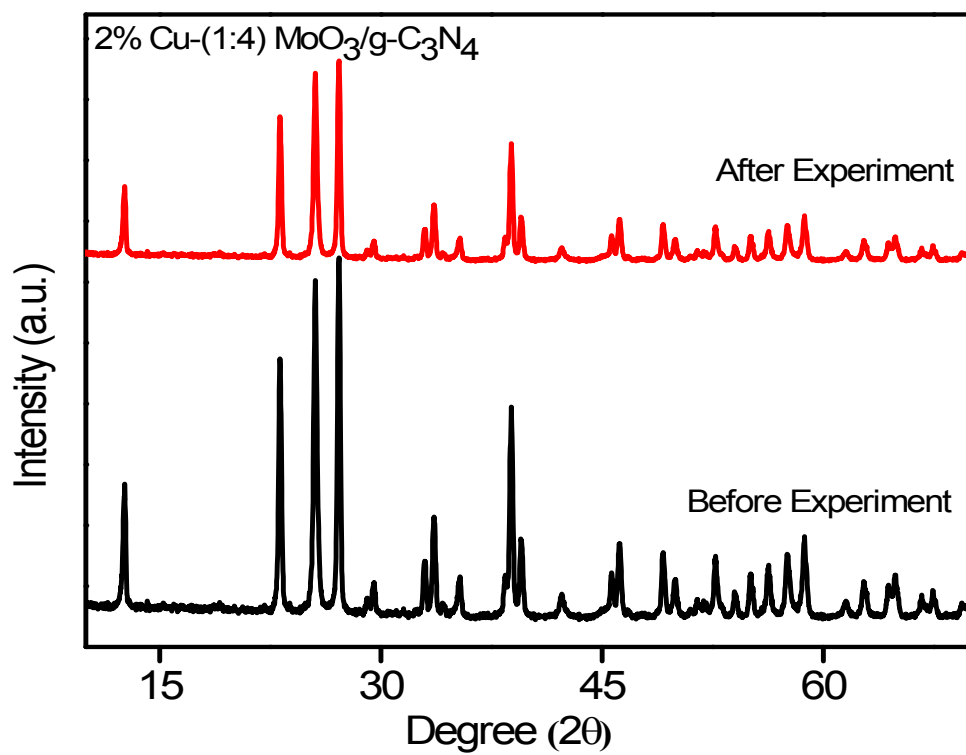


Figure S10. XRD plot of 2% Cu-(1:4) MoO₃/ g-C₃N₄ photocatalyst before and after H₂ evolution experiment

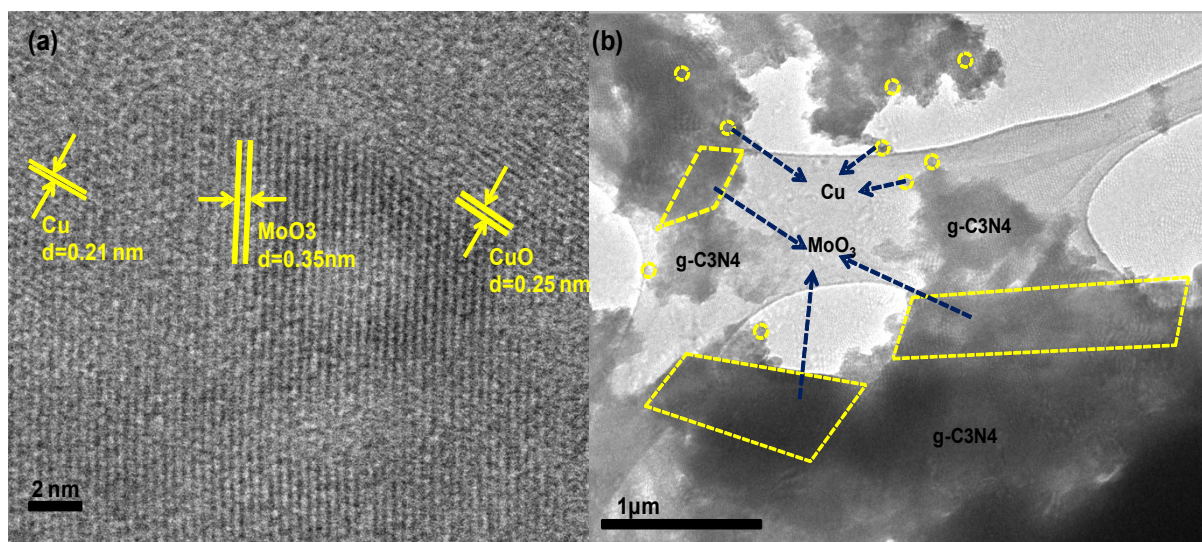


Figure S11. (a) HRTEM and (b) TEM images of 2% Cu-(1:4) MoO₃/g-C₃N₄ photocatalyst after H₂ evolution experiment

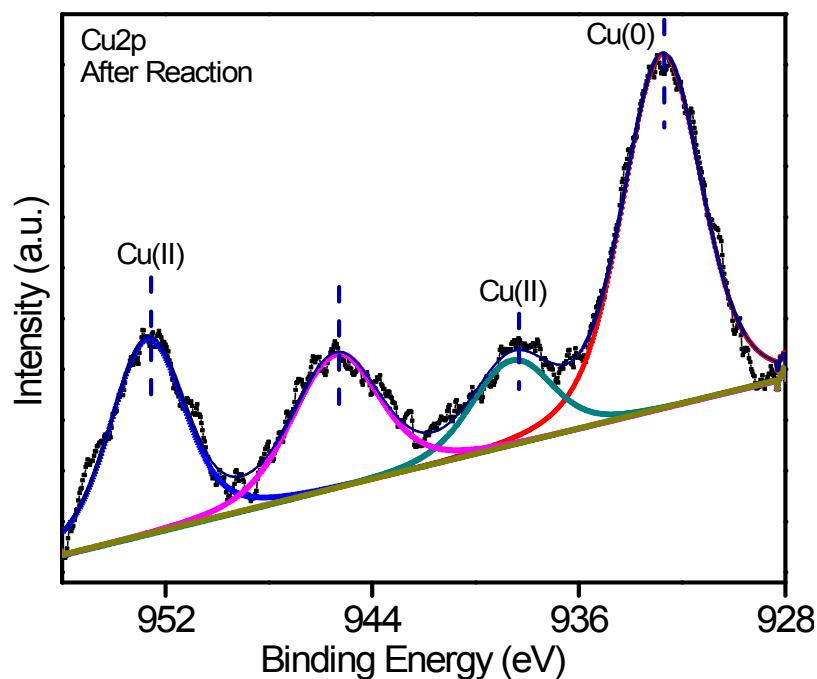


Figure S12. XPS images of 2% Cu-(1:4) MoO₃/ g-C₃N₄ photocatalyst after H₂ evolution experiment

As the enhanced photo activity of the catalyst involves both SPR effect of Cu NPs and shifting of Fermi level of CuO under visible light irradiation both the reactions, $Cu^0 \leftrightarrow Cu^{2+}$ takes place simultaneously. Cu^{2+} ions has tendency to get partially reduced by consuming photo generated electrons and as the photo generated electrons get transferred on to the surface of Cu^0 after equilibration, they also get oxidised to Cu^{2+} . The TEM, HRTEM (Figure S11) and XPS image (Figure S12) of Cu in case of used photo catalyst further confirms the presence of both Cu^0 and Cu^{2+} .

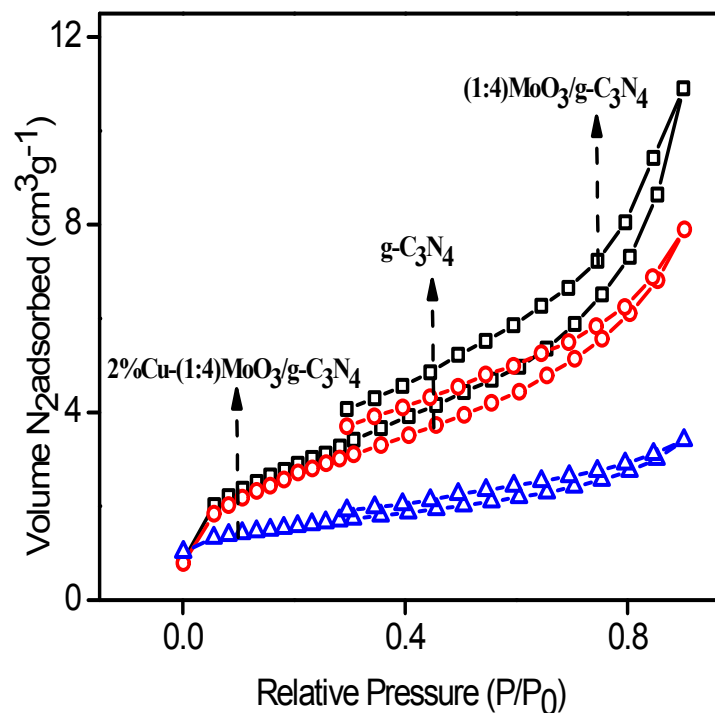


Figure S13. N₂ adsorption and desorption isotherms of g-C₃N₄, (1:4) MoO₃/g-C₃N₄ and Cu-MoO₃/g-C₃N₄ nanocomposite

The details of BET surface areas and pore diameter of g-C₃N₄, (1:4) MoO₃/g-C₃N₄ and Cu-MoO₃/g-C₃N₄ nanocomposites are shown in Table S1 and the isotherms were shown in figure S13. Pure g-C₃N₄ exhibits a lower surface area. However, in situ formation of MoO₃/g-C₃N₄ composite by calcinations method led to the increase in the BET value of photocatalyst, which might be due to the evolution of a number of gases and introduction of porosity. But upon Cu loading the surface area decreases due to pore blockage. Although the surface area decreases, the photo catalytic activity shows an increasing trend owing to increase in the number of active sites and efficient charge separation [7].

Name of the sample	Surface area(m ² g ⁻¹)	Pore volume (cm ³ g ⁻¹)	Pore size (nm)
g-C ₃ N ₄	9.65	0.0122	5.065
(1:4)MoO ₃ /g-C ₃ N ₄	10.7	0.0169	6.311
2%Cu-(1:4) MoO ₃ /g-C ₃ N ₄	2.72	0.0039	5.876

Table S1. Details of surface area and pore volume of g-C₃N₄, (1:4) MoO₃/g-C₃N₄ and Cu-MoO₃/g-C₃N₄

Photocatalyst	Incident light (λ)	Reaction solution	H ₂ Evolution	Conversion Efficiency	Ref
ZnO/ZnS/g-C ₃ N ₄	300 W visible light	0.25 M Na ₂ S/ 0.25 M Na ₂ SO ₃ aq sol ⁿ	1205 $\mu\text{mol/g/4h}$	NA	6
WO ₃ /g-C ₃ N ₄ /Ni(OH) _x	300 W Xe lamp, UV cut-off filter ($\lambda > 400$ nm)	15 vol%TEOA	576 $\mu\text{mol/(g-1 h-1)}$	NA	7
CdS/Au/ g-C ₃ N ₄	$\lambda > 420$ nm	0.1M Na ₂ SO ₄ /0.5 wt. % Pt	19.02 $\mu\text{mol g-1 h-1}$	NA	8
g-C ₃ N ₄ /Au/C-TiO ₂	$\lambda > 420$ nm	TEOA	129.0 $\mu\text{mol g-1 h-1}$	NA	9
g-C ₃ N ₄ /Au/CdZnS	$\lambda > 420$ nm	0.25 M Na ₂ S and 0.35 M Na ₂ SO ₃	6.3 mmol/g in 4h	NA	10
CoTiO ₃ / g-C ₃ N ₄	$\lambda > 420$ nm	10 vol.% ethanol 3 wt.% Pt	858 $\mu\text{mol}\cdot\text{h-1}\cdot\text{g-1}$	38.4% at 365 nm 3.23% at 420 \pm 20 nm	11
Ag ₃ PO ₄ /Ag/ g-C ₃ N ₄	$\lambda > 420$ nm	TEOA	4.1 lmol/gh	NA	12
WO ₃ / g-C ₃ N ₄	$\lambda > 420$ nm	TEOA, 1 wt.% Pt	400 $\mu\text{mol h-1 gcat-1}$	NA	13
g-C ₃ N ₄ /WO ₃	$\lambda > 420$ nm	TEOA, 1 wt.% Pt	2.84 $\mu\text{mol h-1}$	0.9% at 420 nm	14
Cu-MoO ₃ /g-C ₃ N ₄	$\lambda > 420$ nm	10 vol.% Methanol	652 $\mu\text{mol/h}$	Present work	

Table S2 State-of-the-art advancement in the field of Z-scheme photocatalysis for H₂ evolution, NA (Not available)

References

1. N. Sagara, S. Kamimura, T. Tsubota, T. Ohno, *Appl Catal B: Env.*, 2016, **192**, 193–198.
2. M. Wang, S. Shen, L. Li, Z. Tang, and J. Yang, *J. Mater. Sci.*, 2017, **52**, 5155–5164
3. M. R. Gholipour, C. T. Dinh, F. Béland and T. O. Do, *Nanoscale*, 2015, **7**, 8187
4. A. Galin ' ska and J. Walendziewski, *Energy & Fuels*, 2005, **19**, 1143-1147
5. S. Sakthivel, M.V. Shankar, M. Palanichamy, B. Arabindoo, D.W. Bahnemanna and V. Murugesanb, *Water Res.* 2004, **38**, 3001–3008.
6. Z. Dong, Y. Wu, N. Thirugnanam and G. Li, *Applied Sur. Sc.*, 2018, **430**, 293-300
7. M. You, J. Pan, C. Chi, B. Wang, W. Zhao, C. Song, Y. Zheng, and C. Li, *J. Mat. Sci.* 2018, **53**, 1978–1986
8. X. Ding, Y. Li, J. Zhao, Y. Zhu, Y. Li, W. Deng, and C. Wang, *APL MATERIALS* , 2015, **3**, 104410-1
9. Y. Zou, J. W. Shi, D. Ma, Z. Fan, C. Niua and L. Wang, *ChemCatChem*, 2017, **9**, 3752-3761
10. X. Ma, Q. Jiang, W. Guo, M. Zheng, W. Xu, F. Ma, B. Hou, *RSC Adv.*, 2016,**6**, 28263-28269
11. R. Ye, H. B. Fang, Y. Z. Zheng, N. Li, Y. Wang, and X. Tao, *ACS Appl. Mater. Interfaces*, 2016, **8**, 13879–13889
12. M. You, J. Pan, C. Chi, B. Wang, W. Zhao, C. Song, Y. Zheng, and C. Li, *J. Mat. Sci.*, 2018, **53**, 1978-1986
13. C. Cheng, J. Shi, Y. Hu and L. Guo, *Nanotechnology*, 2017, **28**, 164002
14. G. Zhao, X. Huang, F. Fina, G. Zhang and J. T. S. Irvine, *Catal. Sci. Technol.*, 2015, **5**, 3416